Journal of Sound and Vibration (1999) **219**(1), 35–50
Article No. jsvi.1998.1823, available online at http://www.idealibrary.com.on IDEAL

VIBRATION ANALYSIS OF A NEARLY AXISYMMETRIC SHELL STRUCTURE USING A NEW FINITE RING ELEMENT

J. CHUNG

Department of Mechanical Engineering, *Hanyang University*, 1271 *Sa*-1-*dong*, *Ansan*, *Kyunggi-do*, 425-791, *Republic of Korea*

AND

J. M. LEE

Department of Mechanical Design and Production Engineering, *Seoul National University*, *San*-56-1, *Shinlim-dong*, *Kwanak-ku*, *Seoul*, 151-742, *Republic of Korea*

(*Received* 22 *April* 1997, *and in final form* 8 *June* 1998)

A new conical ring element to be used in connection with the finite element method (FEM) is developed, which considers the effects of slight local deviations from an axisymmetric ring. To develop the proposed finite element, the displacements of a point in the ring element are assumed by a pair of the natural modes of a ring with local deviation: symmetric and asymmetric modes. By using the presented finite elements, a FEM program is also developed to analyze free vibrations of a nearly axisymmetric shell structure. The developed program is applied to a vibration analysis of a Korean bell as an example, which shows that the program is very efficient and saves much computation time for shell structures slightly deviating from axisymmetry compared to commercial FEM codes.

1. INTRODUCTION

The vibration analysis of shell structures slightly deviating from perfect axisymmetry is an interesting topic in engineering. For example, slight deviation has aroused great concern in vibration and acoustic analyses of nearly axisymmetric asian bells. It has been shown in investigations that the local deviation causes the bells to have the beat phenomenon which is a unique feature compared to western bells. Other applications of the nearly axisymmetric shell structures can be found in welded cylinders, pressure vessels, tires and so on.

The influence of structural imperfection on thin-walled structures was introduced in the recently published book by Godoy [1]. The main idea behind his presentation is that small imperfections may introduce changes in the stresses due to the loads. Godoy *et al*. [2, 3] also studied the behavior of cylinders with imperfections and investigated the interaction between geometric and intrinsic

0022–460X/99/010035 + 16 $30.00/0

imperfections. On the other hand, many studies have been performed on rings with slight deviation from axisymmetry. Allaei *et al*. [4] studied natural frequencies and mode shapes of a circular ring when the ring is non-axisymmetric due to a mass or stiffness non-uniformity. They also studied natural frequencies and modes of a ring deviating from axisymmetry due to multiple radial springs by using the natural frequencies and modes of the axisymmetric ring [5]. Rossi [6] investigated the in-plane vibrations of a circular ring with a non-uniform cross-section: the natural frequencies and modes were obtained by using the constant-curvature beam finite elements developed by Davis *et al*. [7]. Celep [8] considered the in-plane vibration of a thin ring on a tensionless Winkler foundation. The analysis is based on the harmonic approximation, assuming that the ring is subjected to time dependent in-plane loads. Hong and Lee [9] presented an analytical method to predict the effects of local deviation on the free in-plane vibration of nearly axisymmetric rings. The authors used the Laplace transformation for the solution and the unit step function for the local deviation. They show that, when local deviation is introduced to an axisymmetric ring, the natural modes are separated into the symmetric and asymmetric modes. The symmetric mode has the anti-nodal point at the deviation while the asymmetric mode has the nodal point at the deviation.

In this study, a finite conical ring element with local deviation is developed and a finite element method presented to analyze the natural frequencies and modes of a nearly axisymmetric shell structure with local deviation. The theoretical foundation is based upon the analytical result of Hong and Lee [9]. Furthermore, the effectiveness of the present analysis is shown by applying the method to a Korean bell which is a typical example of a nearly axisymmetric shell structure.

2. CONICAL RING ELEMENT WITH LOCAL DEVIATION

A nearly axisymmetric shell structure with slight deviation is discretized into ring elements as shown in Figure 1. A series of parallel planes perpendicular to the axis of revolution intersect the middle surface of the shell structure. The circles generated by intersection of each plane and the middle surface become the nodal

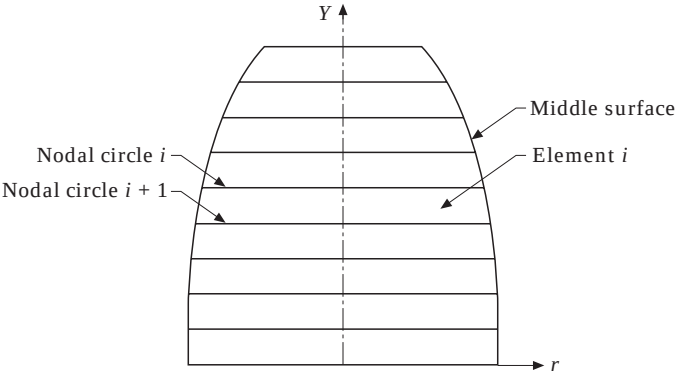

Figure 1. Construction of elements and nodal circles.

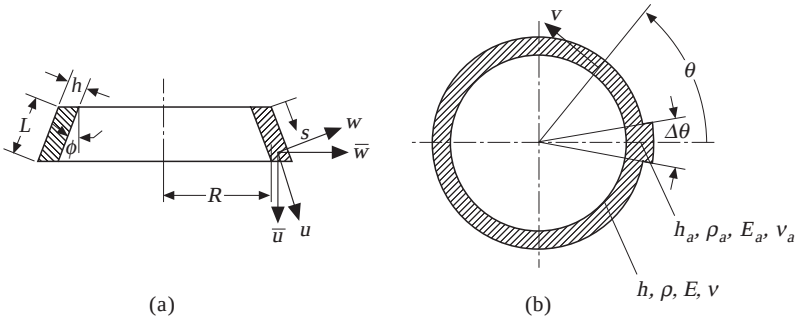

Figure 2. Geometric specification and displacements in the conical ring element.

circles and an element is bounded by two adjacent nodal circles: element i is bounded by nodal circles i and $i+1$. The nodal circle is defined by the radius r and co-ordinate Y.

The geometric specification, displacements and material properties in a conical ring element are shown in Figure 2. The conical ring element is specified by the thickness h, average radius R, slope angle ϕ and the length of the side L. The position of a point in the middle surface of an element is defined by the local meridian coordinate s and the co-ordinate θ. The deviated portion is assumed to be located along $\Delta\theta$ and its thickness is h_a.

3. DISPLACEMENTS IN THE CONICAL RING ELEMENT

The displacements can be described in either the local co-ordinate or global co-ordinate system: u, v and w are the meridian, circumferential and normal displacements in the local co-ordinate system, respectively, while $\bar{u}$, v and $\bar{w}$ are the axial, circumferential and radial displacements in the global co-ordinate system, respectively. Figure 2 shows the displacements defined in the above.

Consider the displacements at a point on the middle surface of an element. Since the meridian, circumferential and normal displacements, u, v and w, are periodic with respect to θ with a period of 2π, they can be expressed in terms of the Fourier series in the θ co-ordinate:

$$u = U_0 + \sum_{j=1}^{n} U_j \cos j\theta + \sum_{j=1}^{n} \bar{U}_j \sin j\theta, \qquad v = V_0 + \sum_{j=1}^{n} V_j \cos j\theta + \sum_{j=1}^{n} \bar{V}_j \sin j\theta, \tag{1, 2}$$

$$w = W_0 + \sum_{j=1}^{n} W_j \cos j\theta + \sum_{j=1}^{n} \bar{W}_j \sin j\theta, \tag{3}$$

where U_j, V_j, W_j, $\bar{U}_j$, $\bar{V}_j$ and $\bar{W}_j$ for $j = 1, 2, \ldots, n$ are functions of the local co-ordinate s. Denoting β as rotation of the meridian, β in the case of the conical ring element can be described as

$$\beta = -\partial w/\partial s \tag{4}$$

Since the heights of the elements are generally small, the meridian contributions of the displacements may be approximated by simple polynomial functions of the meridian co-ordinate s. In this study, linear functions are assumed for the meridian and circumferential displacements and cubic functions are assumed for the normal displacement. That is, U_j, $\bar{U}_j$, V_j and $\bar{V}_j$ are approximated by linear functions while W_j and $\bar{W}_j$ are approximated by cubic functions:

$$U_j = \alpha_{1j} + \alpha_{2j}s, \qquad \bar{U}_j = \bar{\alpha}_{1j} + \bar{\alpha}_{2j}s, \qquad V_j = \alpha_{3j} + \alpha_{4j}s, \qquad \bar{V}_j = \bar{\alpha}_{3j} + \bar{\alpha}_{4j}s, \tag{5–8}$$

$$W_j = \alpha_{5j} + \alpha_{6j}s + \alpha_{7j}s^2 + \alpha_{8j}s^3, \qquad \bar{W}_j = \bar{\alpha}_{5j} + \bar{\alpha}_{6j}s + \bar{\alpha}_{7j}s^2 + \bar{\alpha}_{8j}s^3. \tag{9, 10}$$

It is assumed in this paper that the mode shapes of the ring element with slight asymmetry are known. As mentioned in the Introduction, Hong and Lee [9] showed that due to local deviation a ring has the natural modes which can be separated into symmetric and asymmetric modes. Local deviation is located on an anti-nodal point of the symmetric mode while it is located on a nodal point of the asymmetric mode. This means that, for each harmonic number j, the asymmetric mode shape rotates with $\pi/2j$ from the symmetric mode shape. For example, the asymmetric mode shape rotates with 45° from the symmetric one for $j = 2$. Under the assumption, the displacements given by equations (1–3) might be replaced with the mode shapes of the conical ring element with slight deviation in order to derive the eigenproblem of the nearly axisymmetric shell structure with slight deviation:

$$u = (\alpha_1 + \alpha_2 s)\cos(j\theta - \pi b/2), \qquad v = (\alpha_3 + \alpha_4 s)\sin(j\theta - \pi b/2), \tag{11, 12}$$

$$w = (\alpha_5 + \alpha_6 s + \alpha_7 s^2 + \alpha_8 s^3)\cos(j\theta - \pi b/2), \qquad \beta = -\partial w/\partial s, \tag{13, 14}$$

in which α_i's for $i = 1, 2, \ldots, 8$ are constants to be determined and b is the parameter related to the symmetric and asymmetric modes. The symmetric mode corresponds to $b = 0$ while the asymmetric mode corresponds to $b = 1$. In order to perform the analysis, it is convenient to express the mode shapes of the ring in a vector matrix equation

$$\mathbf{u} = \mathbf{H}_s \mathbf{p}_\alpha \boldsymbol{\alpha}, \tag{15}$$

where

$$\mathbf{u} = \left\{u, v, w, \frac{\partial w}{\partial s}\right\}^{\mathrm{T}}, \qquad \mathbf{p}_\alpha = \begin{bmatrix} 1 & s & 0 & 0 & 0 & 0 & 0 & 0 \\ 0 & 0 & 1 & s & 0 & 0 & 0 & 0 \\ 0 & 0 & 0 & 0 & 1 & s & s^2 & s^3 \\ 0 & 0 & 0 & 0 & 0 & 1 & 2s & 3s^2 \end{bmatrix}, \tag{16, 17}$$

$$\boldsymbol{\alpha} = \{\alpha_1, \alpha_2, \alpha_3, \alpha_4, \alpha_5, \alpha_6, \alpha_7, \alpha_8\}^{\mathrm{T}}, \qquad \mathbf{H}_s = \begin{bmatrix} C_j(\theta) & 0 & 0 & 0 \\ 0 & S_j(\theta) & 0 & 0 \\ 0 & 0 & C_j(\theta) & 0 \\ 0 & 0 & 0 & C_j(\theta) \end{bmatrix} \tag{18, 19}$$

in which

$$C_j(\theta) = \cos(j\theta - \pi b/2), \qquad S_j(\theta) = \sin(j\theta - \pi b/2). \tag{20, 21}$$

The displacements in the conical ring element can be expressed by the displacements on the nodal circles that bound the element. At a given value of θ, e.g., θ_0, the displacement vector $\mathbf{u}$ is given by

$$\mathbf{u}|_{\theta=\theta_0} = \mathbf{H}_s|_{\theta=\theta_0}\mathbf{p}_\alpha\alpha. \tag{22}$$

Let u_i, v_i, w_i and $(\partial w/\partial s)_i$ be the displacements on nodal circle i at $\theta = \theta_0$ and let u_{i+1}, v_{i+1}, w_{i+1} and $(\partial w/\partial s)_{i+1}$ be the displacements on nodal circle $i+1$ at $\theta = \theta_0$. Then the nodal displacement vector, at $\theta = \theta_0$, can be expressed as

$$\mathbf{U}_e = \begin{bmatrix} \mathbf{H}_s|_{\theta=\theta_0} & \mathbf{0} \\ \mathbf{0} & \mathbf{H}_s|_{\theta=\theta_0} \end{bmatrix}\mathbf{P}\boldsymbol{\alpha}, \tag{23}$$

where

$$\mathbf{U}_e = \left\{u_i, v_i, w_i, \left(\frac{\partial w}{\partial s}\right)_i, u_{i+1}, v_{i+1}, w_{i+1}, \left(\frac{\partial w}{\partial s}\right)_{i+1}\right\}^{\mathrm{T}}, \qquad \mathbf{P} = \begin{bmatrix} \mathbf{P}_\alpha|_{s=0} \\ \mathbf{P}_\alpha|_{s=L} \end{bmatrix}_{8\times 8} \tag{24, 25}$$

Solving equation (23) for $\boldsymbol{\alpha}$ and substituting $\boldsymbol{\alpha}$ into equation (22), the displacements in the ring are given by

$$\mathbf{u}|_{\theta=\theta_0} = \mathbf{S}\mathbf{U}_e, \tag{26}$$

where $\mathbf{S}$ may be simplified as

$$\mathbf{S} = \mathbf{p}_\alpha\mathbf{P}^{-1}, \tag{27}$$

and $\mathbf{S}$ is called the 4×8 displacement interpolation matrix (see the Appendix for $\mathbf{S}$). Consequently, the displacement vector $\mathbf{u}$ corresponding to the mode shape of the conical ring is represented with respect to the nodal displacement vector $\mathbf{U}_e$:

$$\mathbf{u} = \mathbf{H}_S\mathbf{S}\mathbf{U}_e \tag{28}$$

When assembling the element mass and stiffness matrices to those of the global matrices, the global description is more suitable than the local description; therefore, the displacements u_i, v_i, w_i, $(\partial w/\partial s)_i$, u_{i+1}, v_{i+1}, w_{i+1} and $(\partial w/\partial s)_{i+1}$ in

the local co-ordinate system must be transformed to $\bar{u}_i$, v_i, $\bar{w}_i$, $(\partial w/\partial s)_i$, $\bar{u}_{i+1}$, v_{i+1}, $\bar{w}_{i+1}$ and $(\partial w/\partial s)_{i+1}$ in the global co-ordinate system (see Figure 2):

$$\bar{\mathbf{U}}_e = \mathbf{T}_e \mathbf{U}_e \tag{29}$$

where

$$\bar{\mathbf{U}}_e = \{\bar{u}_i, v_i, \bar{w}_i, (\partial w/\partial s)_i, \bar{u}_{i+1}, v_{i+1}, \bar{w}_{i+1}, (\partial w/\partial s)_{i+1}\}^{\mathrm{T}}, \tag{30}$$

$$\mathbf{T}_e = \begin{bmatrix} \cos\phi & 0 & -\sin\phi & 0 & 0 & 0 & 0 & 0 \\ 0 & 1 & 0 & 0 & 0 & 0 & 0 & 0 \\ \sin\phi & 0 & \cos\phi & 0 & 0 & 0 & 0 & 0 \\ 0 & 0 & 0 & 1 & 0 & 0 & 0 & 0 \\ 0 & 0 & 0 & 0 & \cos\phi & 0 & -\sin\phi & 0 \\ 0 & 0 & 0 & 0 & 0 & 1 & 0 & 0 \\ 0 & 0 & 0 & 0 & \sin\phi & 0 & \cos\phi & 0 \\ 0 & 0 & 0 & 0 & 0 & 0 & 0 & 1 \end{bmatrix} \tag{31}$$

Since $\mathbf{U}_e = \mathbf{T}_e^{\mathrm{T}} \bar{\mathbf{U}}_e$ from equation (29), equation (28) can be rewritten as

$$\mathbf{u} = \mathbf{H}_S \mathbf{S} \mathbf{T}_e^{\mathrm{T}} \bar{\mathbf{U}}_e \tag{32}$$

where $\mathbf{H}_S \mathbf{S} \mathbf{T}_e^{\mathrm{T}}$ is the 4×8 displacement interpolation matrix.

4. RELATIONS BETWEEN THE DISPLACEMENTS, STRAINS AND STRESS RESULTANTS

Various strain–displacement relationships may be obtained from the well-known strain–displacement equations of the three-dimensional theory of elasticity, depending upon the type of shell element employed. This study adopts the strain–displacement relationships of the Sanders–Koiter theory described by Morris [10]. In the theory the strains and curvature changes on the middle surface of the axisymmetric shell are defined by

$$\epsilon_s = \partial u/\partial s - w\,\partial\phi/\partial s, \qquad \epsilon_\theta = (1/r)(u\sin\phi + \partial v/\partial\theta + w\cos\phi), \tag{33, 34}$$

$$\epsilon_{s\theta} = \partial u/r\,\partial\theta - v\sin\phi/r + \partial v/\partial s, \qquad \chi_s = -(\partial u/\partial s)\,\partial\phi/\partial s - u\,\partial^2\phi/\partial s^2 - \partial^2 w/\partial s^2, \tag{35, 36}$$

$$\chi_\theta = -(u\sin\phi/r)\,\partial\phi/\partial s + (\cos\phi/r^2)\,\partial v/\partial\theta - \partial^2 w/r^2\,\partial\theta^2 - (\sin\phi/r)\,\partial w/\partial s, \tag{37}$$

$$\chi_{s\theta} = -\partial^2 w/r\,\partial s\,\partial\theta + (\sin\phi/r^2)\,\partial w/\partial\theta - (\tfrac{1}{4}\cos\phi/r + \tfrac{3}{4}\,\partial\phi/\partial s)\,\partial u/r\,\partial\theta - (\tfrac{3}{4}\cos\phi/r + \tfrac{1}{4}\,\partial\phi/\partial s)((\sin\phi/r)v - \partial v/\partial s), \tag{38}$$

where ϵ_s, ϵ_θ and $\epsilon_{s\theta}$ are the normal and shear strains at an arbitrary point on the middle surface; χ_s and χ_θ are the curvature changes of the middle surface; $\chi_{s\theta}$ is the middle surface twist. Since the conical ring element has a constant value of ϕ, the derivatives of ϕ with respect to s become zero. Moreover, if it is assumed

that the heights of the elements are small enough, r in equations (33–38) can be replaced by the average radius of the conical ring element R. In this case, the strain–displacement relationships are simplified as follows:

$$\epsilon_s = \partial u/\partial s, \qquad \epsilon_\theta = (1/R)(u \sin\phi + \partial v/\partial\theta + w\cos\phi), \tag{39, 40}$$

$$\epsilon_{s\theta} = \partial u/R\,\partial\theta - v\sin\phi/R + \partial v/\partial s, \tag{41}$$

$$\chi_s = -\partial^2 w/\partial s^2, \qquad \chi_\theta = (\cos\phi/R^2)\,\partial v/\partial\theta - \partial^2 w/R^2\,\partial\theta^2 - (\sin\phi/R)\,\partial w/\partial s, \tag{42, 43}$$

$$\chi_{s\theta} = -\partial^2 w/R\,\partial s\,\partial\theta + (\sin\phi/R^2)\,\partial w/\partial\theta - \tfrac{1}{4}(\cos\phi/R^2)\,\partial u/\partial\theta - \tfrac{3}{4}(\cos\phi/R)((\sin\phi/R)v - \partial v/\partial s). \tag{44}$$

In order that the strains are expressed with respect to the nodal displacements, it is required that equations (39–44) should be written in a matrix vector equation and then equation (32) should be substituted into the equation. In this case, the strain vector can be expressed as

$$\boldsymbol{\epsilon} = \mathbf{H}_B\mathbf{B}\mathbf{T}_e^{\mathrm{T}}\bar{\mathbf{U}}, \tag{45}$$

where

$$\boldsymbol{\epsilon} = \{\epsilon_s, \epsilon_\theta, \epsilon_{s\theta}, \chi_s, \chi_\theta, \chi_{s\theta}\}^{\mathrm{T}} \tag{46}$$

$$\mathbf{H}_B = \begin{bmatrix} C_j(\theta) & 0 & 0 & 0 & 0 & 0 \\ 0 & C_j(\theta) & 0 & 0 & 0 & 0 \\ 0 & 0 & S_j(\theta) & 0 & 0 & 0 \\ 0 & 0 & 0 & C_j(\theta) & 0 & 0 \\ 0 & 0 & 0 & 0 & C_j(\theta) & 0 \\ 0 & 0 & 0 & 0 & 0 & S_j(\theta) \end{bmatrix}, \tag{47}$$

and $\mathbf{B}$ is the 6×8 matrix which is a function of s, which is shown in the Appendix.

The stress resultants and stress couples, for the thickness h, are related to the strains and curvature changes at the middle surface through the elastic matrix $\mathbf{D}$. The stress resultant vector is given by

$$\mathbf{N} = \mathbf{D}\boldsymbol{\epsilon}, \tag{48}$$

where

$$\mathbf{N} = \{N_s, N_\theta, N_{s\theta}, M_s, M_\theta, M_{s\theta}\}^{\mathrm{T}}, \tag{49}$$

in which N_s, N_θ and $N_{s\theta}$ are the stress resultants and M_s, M_θ and $M_{s\theta}$ are the stress couples. For shells with a homogeneous elastic Hookean material, the elastic matrix is given by

$$\mathbf{D} = \begin{bmatrix} C & vC & 0 & 0 & 0 & 0 \\ vC & C & 0 & 0 & 0 & 0 \\ 0 & 0 & (1-v)C/2 & 0 & 0 & 0 \\ 0 & 0 & 0 & D & vD & 0 \\ 0 & 0 & 0 & vD & D & 0 \\ 0 & 0 & 0 & 0 & 0 & (1-v)D/2 \end{bmatrix}, \tag{50}$$

where E and v are Young's modulus and Poisson's ratio, respectively; $D = Eh^3/12(1-v^2)$ is the bending stiffness and $C = Eh/(1-v^2)$ is the extensional stiffness.

5. EQUATION OF MOTION IN MATRIX VECTOR FORM

The equation of motion for free vibration can be derived by using Hamilton's principle which is described by

$$\delta \int_{t_0}^{t_1} (T - U)\, \mathrm{d}t = 0, \tag{51}$$

where T and U are the total kinetic and strain energies; t_0 and t_1 are arbitrary time. Suppose that a shell structure is discretized into N conical ring elements. Since the total kinetic and strain energies are the summation of those of the N elements and the variation operator δ is independent of the integration, equation (51) can be rewritten as

$$\sum_{e=1}^{N} \int_{t_0}^{t_1} (\delta T_e - \delta U_e)\, \mathrm{d}t = 0, \tag{52}$$

where T_e and U_e are the element kinetic and strain energies.

The variation of the kinetic energy of an element is given by

$$\delta T_e = \int_V \rho \dot{\mathbf{u}}^{\mathrm{T}}\, \delta \dot{\mathbf{u}}\, \mathrm{d}V, \tag{53}$$

where V and ρ are the volume and density of an element, respectively. Integrating equation (53) by parts with respect to time t, equation (53) is written as

$$\int_{t_0}^{t_1} \delta T_e\, \mathrm{d}t = -\int_{t_0}^{t_1} \int_V \rho \ddot{\mathbf{u}}^{\mathrm{T}}\, \delta \mathbf{u}\, \mathrm{d}V\, \mathrm{d}t. \tag{54}$$

Substitution of equation (32) into equation (54) leads to

$$\int_{t_0}^{t_1} \delta T_e \, \mathrm{d}t = -\int_{t_0}^{t_1} \delta \bar{\mathbf{U}}_e^{\mathrm{T}} \mathbf{M}_e \ddot{\bar{\mathbf{U}}}_e \, \mathrm{d}t, \tag{55}$$

where $\mathbf{M}_e$ is the 8×8 symmetric element mass matrix given by

$$\mathbf{M}_e = \int_V \mathbf{T}_e \mathbf{S}^{\mathrm{T}} \mathbf{H}_S \rho \mathbf{H}_S \mathbf{S} \mathbf{T}_e^{\mathrm{T}} \, \mathrm{d}V. \tag{56}$$

On the other hand, the variation of the element strain energy U_e is given by

$$\delta U_e = \int_A \mathbf{N}^{\mathrm{T}} \, \delta \boldsymbol{\epsilon} \, \mathrm{d}A, \tag{57}$$

where A is the area of the middle surface for the ring element. Using equations (45) and (48), equation (57) may be rewritten as

$$\delta U_e = \delta \bar{\mathbf{U}}_e^{\mathrm{T}} \mathbf{K}_e \bar{\mathbf{U}}_e, \tag{58}$$

where $\mathbf{K}_e$ is the 8×8 symmetric element stiffness matrix given by

$$\mathbf{K}_e = \int_A \mathbf{T}_e \mathbf{B}^{\mathrm{T}} \mathbf{H}_B \mathbf{D} \mathbf{H}_B \mathbf{B} \mathbf{T}_e^{\mathrm{T}} \, \mathrm{d}A \tag{59}$$

Substituting equations (55) and (58) into equation (52), equation (52) becomes

$$\sum_{e=1}^{N} \int_{t_0}^{t_1} \delta \bar{\mathbf{U}}_e^{\mathrm{T}} (\mathbf{M}_e \ddot{\bar{\mathbf{U}}}_e + \mathbf{K}_e \bar{\mathbf{U}}_e) \, \mathrm{d}t = 0. \tag{60}$$

Since equation (60) is valid for arbitrary variation $\delta \bar{\mathbf{U}}_e^{\mathrm{T}}$, vanishing the coefficient of $\delta \bar{\mathbf{U}}_e^{\mathrm{T}}$ leads to the global matrix vector equation:

$$\mathbf{M} \ddot{\bar{\mathbf{U}}} + \mathbf{K} \bar{\mathbf{U}} = \mathbf{0}, \tag{61}$$

where $\mathbf{M}$ and $\mathbf{K}$ are the $4(N+1) \times 4(N+1)$ global mass and stiffness matrices, respectively, and $\bar{\mathbf{U}}$ is the $4(N+1) \times 1$ displacement vector in the global co-ordinate system, given by

$$\bar{\mathbf{U}} = \{\bar{u}_1, v_1, \bar{w}_1, (\partial w/\partial s)_1, \bar{u}_2, v_2, \bar{w}_2, (\partial w/\partial s)_2, \ldots, \bar{u}_{N+1}, v_{N+1}, \bar{w}_{N+1}, (\partial w/\partial s)_{N+1}\}^{\mathrm{T}}. \tag{62}$$

The boundary conditions may be imposed on equation (61) in the sense of the penalty method.

6. COMPUTATION OF THE ELEMENT MASS AND STIFFNESS MATRICES

Consider first the computation of the element mass matrix for the conical ring element with slight deviation. Note that $\mathbf{T}_e$ is independent of θ and s, $\mathbf{S}$ is a function of s, and $\mathbf{H}_s$ is a function of θ. When introducing a parametric co-ordinate p defined by

$$p = 2s/L - 1, \tag{63}$$

$\mathbf{S}$ becomes a function of p. Then, the element mass matrix of equation (56) may be expressed as

$$\mathbf{M}_e = \tfrac{1}{2}RL\mathbf{T}_e\left(\int_{-1}^{1} \mathbf{S}^{\mathrm{T}}\mathbf{G}_M\mathbf{S}\,\mathrm{d}p\right)\mathbf{T}_e^{\mathrm{T}}, \tag{64}$$

where

$$\mathbf{G}_M = \pi\rho h\mathbf{I} - (\rho h - \rho_a h_a)(A\mathbf{I} - B\mathbf{T}_M), \tag{65}$$

in which $\mathbf{I}$ is the 4×4 identity matrix; ρ_a and h_a are the density and thickness of the deviated portion of the ring while ρ and h are the density and thickness of the other portion, respectively (see Figure 2);

$$\mathbf{T}_M = \begin{bmatrix} 1 & 0 & 0 & 0 \\ 0 & -1 & 0 & 0 \\ 0 & 0 & 1 & 0 \\ 0 & 0 & 0 & 1 \end{bmatrix}, \qquad A = \tfrac{1}{2}\Delta\theta, \qquad B = [(-1)^b/2j]\sin j\Delta\theta. \tag{64–66}$$

Similarly, since $\mathbf{B}$ is a function of s or p and $\mathbf{H}_B$ is a function of θ, the element stiffness matrix can be written as

$$\mathbf{K}_e = \tfrac{1}{2}RL\mathbf{T}_e\left(\int_{-1}^{1} \mathbf{B}^{\mathrm{T}}\mathbf{G}_K\mathbf{B}\,\mathrm{d}p\right)\mathbf{T}_e^{\mathrm{T}}, \tag{67}$$

where

$$\mathbf{G}_K = \pi\mathbf{D} - (A\mathbf{I} + B\mathbf{T}_K)(\mathbf{D} - \mathbf{D}_a) \tag{68}$$

in which $\mathbf{I}$ is the 6×6 identity matrix and $\mathbf{D}_a$ is the elastic matrix for the deviated portion;

$$\mathbf{T}_K = \begin{bmatrix} 1 & 0 & 0 & 0 & 0 & 0 \\ 0 & 1 & 0 & 0 & 0 & 0 \\ 0 & 0 & -1 & 0 & 0 & 0 \\ 0 & 0 & 0 & 1 & 0 & 0 \\ 0 & 0 & 0 & 0 & 1 & 0 \\ 0 & 0 & 0 & 0 & 0 & -1 \end{bmatrix}, \tag{69}$$

The Gaussian quadrature is used to integrate $\mathbf{S}^T\mathbf{G}_M\mathbf{S}$ and $\mathbf{B}^T\mathbf{G}_K\mathbf{B}$ with respect to p from -1 to 1. Note that the elements in $\mathbf{S}$ and $\mathbf{B}$ are polynomials of p with the highest degree 3. If the thickness h is approximated by a linear polynomial of s or p, the elements in $\mathbf{D}$ become polynomials of p with degree 3. Since the highest degrees of the elements in $\mathbf{S}^T\mathbf{G}_M\mathbf{S}$ and $\mathbf{B}^T\mathbf{G}_K\mathbf{B}$ are 7 and 9, respectively, the 4-point Gaussian quadrature gives exact values of integration for $\mathbf{M}_e$ and $\mathbf{K}_e$.

7. COMPUTATION OF NATURAL FREQUENCIES AND MODES

Natural frequencies and mode shapes of a nearly axisymmetric shell structure are obtained from the eigenproblem, corresponding to equation (61), that is given by

$$(\mathbf{K} - \omega_n^2\mathbf{M})\mathbf{X} = \mathbf{0} \tag{70}$$

where ω_n is the natural frequency and $\mathbf{X}$ is the eigenvector.

To demonstrate the computational efficiency of the proposed approach, let us consider the nearly axisymmetric shell structure of a Korean bell as an example. The material properties of the bell are $\rho = 8800\,\text{kg/m}^3$, $E = 100\,\text{GN/m}^2$ and $v = 0{\cdot}33$. The discretized model for the FEM is shown in Figure 3 where the numbers are element numbers of the ring elements. All the elements are axisymmetric except elements 15, 16 and 17. These three elements have the local deviations which are defined by $\Delta\theta = 20^\circ$ and $h_a = 1{\cdot}1h$ as shown in Figure 2. Since element i is bounded by nodal circles i and $i + 1$, the element–node connectivity is given in Table 1 where h_i and h_{i+1} represent the thickness at nodal circles i and $i + 1$, respectively, and γ_h is defined as $\gamma_h = (h_a - h)/h$. Table 2 shows the co-ordinates of the nodal circles. The fixed boundary conditions are imposed on nodal circle 1 so that all the displacements are equal to zero at the circle.

The computation results from the proposed method are summarized and compared to those from a commercial code ANSYS [11] in Table 3 which presents

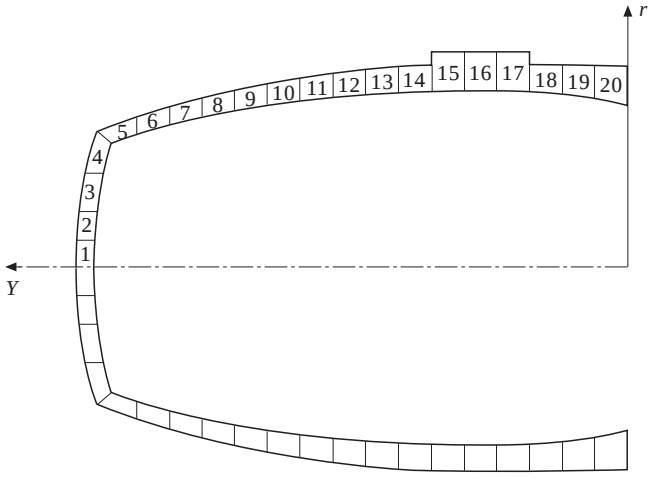

Figure 3. Discretized model of the nearly axisymmetric shell structure.

TABLE 1

Element-node connectivity, element thickness, and deviations from symmetry

Element no. (i)	Nodal Circle i	Nodal Circle $i+1$	h_i (cm)	h_{i+1} (cm)	γ_h (%)	$\Delta\theta$ (deg)
1	1	2	11·50	11·50	0·00	0·00
2	2	3	11·50	11·70	0·00	0·00
3	3	4	11·70	11·50	0·00	0·00
4	4	5	11·50	11·30	0·00	0·00
5	5	6	11·30	11·20	0·00	0·00
6	6	7	11·20	11·28	0·00	0·00
7	7	8	11·28	11·98	0·00	0·00
8	8	9	11·98	12·90	0·00	0·00
9	9	10	12·90	13·51	0·00	0·00
10	10	11	13·51	14·21	0·00	0·00
11	11	12	14·21	14·76	0·00	0·00
12	12	13	14·76	15·11	0·00	0·00
13	13	14	15·11	15·68	0·00	0·00
14	14	15	15·68	16·15	0·00	0·00
15	15	16	16·15	16·78	10·0	20·0
16	16	17	16·78	16·67	10·0	20·0
17	17	18	16·67	16·80	10·0	20·0
18	18	19	16·80	17·37	0·00	0·00
19	19	20	17·37	19·48	0·00	0·00
20	20	21	19·48	20·12	0·00	0·00

the lowest eight natural frequencies except the natural frequencies corresponding to the rigid-body modes. In Table 3, the mode (m, n) represents a mode which has m nodal points along the circumference of the shell and $n + 1$ nodal points along the meridian of the shell. See Figure 4 for the mode shapes. Note that $m = 2j$ where j is the harmonic number shown in equations (1–3). It is also noted that since the

TABLE 2

Co-ordinates of the nodal circles

Nodal circle i	r_i (cm)	Y_i (cm)	Nodal circle i	r_i (cm)	Y_i (cm)
1	0·00	334·25	12	113·55	181·50
2	17·90	333·95	13	115·75	161·40
3	35·60	332·45	14	117·25	141·20
4	59·20	328·75	15	118·20	121·00
5	81·40	322·85	16	118·50	100·90
6	88·30	302·60	17	118·15	80·70
7	94·25	282·40	18	117·75	60·50
8	99·30	262·20	19	117·30	40·30
9	103·75	242·20	20	115·75	20·20
10	107·55	221·90	21	113·60	0·00
11	110·90	201·70			

TABLE 3

Computed natural frequencies from the proposed method and ANSYS (Hz)

Number of elements	Mode (4, 0)		Mode (6, 0)		Mode (4, 1)		Mode (6, 1)	
	$b = 0$	$b = 1$	$b = 0$	$b = 1$	$b = 0$	$b = 1$	$b = 0$	$b = 1$
10	59·18	59·71	162·28	164·84	173·12	173·47	210·33	210·37
20	60·26	60·58	165·89	166·56	171·02	171·19	210·86	210·92
40	60·66	60·89	166·30	166·55	170·66	170·81	211·33	211·54
ANSYS	60·71	60·82	165·96	166·48	174·94	175·41	223·75	224·29

modes (2, 0) and (2, 1) correspond to the rigid-body modes, the natural frequencies for those modes are equal to zero theoretically. Actual computation shows that these frequencies are equal to 0·03 and 0·06. However, because the rigid-body modes are not important, they are omitted in Table 3. For the given values of m and n, each mode (m, n) is separated into the symmetric mode ($b = 0$) and asymmetric mode ($b = 1$).

The natural frequencies computed using 10, 20 and 40 elements show the convergence of the method and they are close to those computed by ANSYS. Considering the deviation from axisymmetry for the given structure, the FEM model for ANSYS has 1446 three-dimensional structural solid elements named by SOLID45; however, the model for the proposed method has at most 40 ring elements. On the other hand, the computation time is 699·37 s when ANSYS runs on a workstation while the computation time is only 3·15 and 5·61 s with 20 and 40 elements respectively when the proposed FEM program runs on a 586 personal computer. In practice, the frequencies corresponding to the mode (4, 0) are

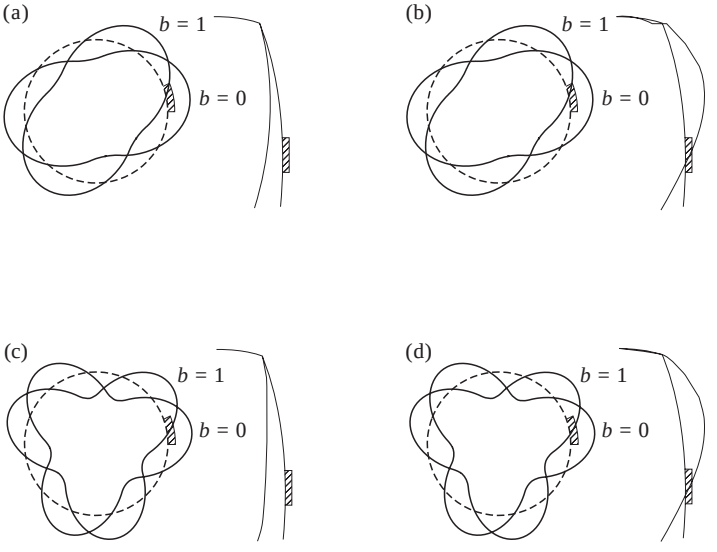

Figure 4. Mode shapes of the nearly axisymmetric shell structure: (a) Mode (4, 0); (b) mode (4, 1); (c) mode (6, 0); (d) mode (6, 1).

important in the design of Korean bells because the fundamental beat frequencies are dominant in determining sound quality. In addition, iteration of computation for the fundamental frequencies is required in the design stage of Korean bells; therefore, the proposed approach is very useful because a large amount of computation time and cost can be saved compared to that of commercial FEM codes.

The mode shapes of the above structure are plotted in Figure 4. The modes denoted by $b = 0$ and $b = 1$ are the symmetric and asymmetric modes, respectively. The hatched parts represent the added mass, i.e., the deviation from axisymmetry of the structure. The circumferential mode patterns show that the deviated part is located on the anti-node of the symmetric mode while it is located on the node of the asymmetric mode. Finally, one can see that modes (4, 1) and (6, 1) have the meridian mode patterns which pass the deviation part.

8. CONCLUSIONS

The new conical ring finite element with local deviation is developed, based upon the fact that the deviation generates the beat frequencies and the fact that, for each harmonic number j, the asymmetric mode shape rotates with $\pi/2j$ from the symmetric mode shape. The developed element is applied to the FEM program which computes natural frequencies and mode shapes for the nearly axisymmetric shell structure. The example of the Korean bell shows that the finite element method using the proposed elements can save a great deal of computation time and cost. The present finite element analysis may be applied to welded cylinders and pressure vessels.

REFERENCES

1. L. A. Godoy 1996 *Thin-Walled Structures With Structural Imperfections*: *Analysis and Behavior*. Oxford: Pergamon.
2. L. A. Godoy, J. G. A. Croll and K. O. Kemp 1985 *Journal of Strain Analysis* **20**, 15–22. Stresses in axially loaded cylinders with imperfections and cracks.
3. L. A. Godoy, J. G. A. Croll, K. O. Kemp and J. F. Jackson 1981 *Journal of Strain Analysis* **16**, 59–65. An experimental study of the stresses in a shell of revolution with geometrical imperfections and cracks.
4. D. Allaei, W. Soedel and T. Y. Yang 1986 *Journal of Sound and Vibration* **111**, 9–27. Natural frequencies and modes of rings that deviate from perfect axisymmetry.
5. D. Allaei, W. Soedel and T. Y. Yang 1987 *Journal of Sound and Vibration* **121**, 547–561. Eigenvalues of rings with radial spring attachments.
6. R. E. Rossi 1989 *Journal of Sound and Vibration* **135**, 443–452. In-plane vibrations of circular rings of non-uniform cross-section with account taken of shear and rotatory inertia effects.
7. R. Davis, R. H. Henshell and G. B. Warburton 1972 *Journal of Sound and Vibration* **25**, 561–576. Constant curvature beam finite elements for in-plane vibration.
8. Z. Celep 1990 *Journal of Sound and Vibration* **121**, 547–561. In-plane vibrations of circular rings on a tensionless foundation.
9. J. S. Hong and J. M. Lee 1994 *ASME Journal of Applied Mechanics* **61**, 317–322. Vibration of circular ring with local deviation.
10. D. G. Ashwell and R. H. Gallagher 1976 *Finite Elements for Thin Shells and Curved Members*. Chichester: John Wiley.
11. Swanson Analysis Co. 1996 *ANSYS User's Manual*, Version 5.1.

$$\mathbf{S} = \begin{bmatrix} (L-s)/L & 0 & 0 & 0 & s/L & 0 & 0 & 0 \\ 0 & (L-s)/L & 0 & 0 & 0 & s/L & 0 & 0 \\ 0 & 0 & (L-s)^2(L+2s)/L^3 & (L-s)^2 s/L^2 & 0 & 0 & (3L-2s)s^2/L^3 & -(L-s)s^2/L^2 \\ 0 & 0 & -6(L-s)s/L^3 & (L-3s)(L-s)/L^2 & 0 & 0 & 6(L-s)s/L^3 & -(2L-3s)s/L^2 \end{bmatrix}$$

$$b_{12} = b_{13} = b_{14} = b_{16} = b_{17} = b_{18} = b_{33} = b_{34} = b_{37} = b_{38} = 0,$$

$$b_{41} = b_{42} = b_{45} = b_{46} = b_{51} = b_{55} = 0,$$

$$b_{11} = -b_{15} = -1/L, \qquad b_{21} = (\sin\phi/RL)(L-s),$$
$$b_{22} = -b_{31} = (j/RL)(L-s),$$

$$b_{23} = (\cos\phi/RL^3)(L-s)^2(L+2s), \qquad b_{24} = (\cos\phi/RL^2)(L-s)^2 s,$$

$$b_{25} = (\sin\phi/RL)s,$$

$$b_{26} = -b_{35} = (j/RL)s, \qquad b_{27} = (\cos\phi/RL^3)(3L-2s)s^2,$$

$$b_{28} = -(\cos\phi/RL^2)(L-s)s^2,$$

$$b_{32} = -(\sin\phi/RL)(L-s) - 1/L, \qquad b_{36} = -(\sin\phi/RL)s + 1/L,$$

$$b_{43} = -b_{47} = -(6/L^3)(L-2s), \qquad b_{44} = (2/L^2)(2L-3s), \qquad b_{48} = (2/L^2)(L-3s),$$

$$b_{52} = 4b_{61} = (j\cos\phi/R^2L)(L-s),$$

$$b_{53} = (6\sin\phi/RL^3)(L-s)s + (j^2/R^2L^3)(L-s)^2(L+2s),$$

$$b_{54} = (\sin\phi/RL^2)(L-3s)(L-s) + (j^2/R^2L^2)(L-s)^2 s,$$

$$b_{56} = 4b_{65} = (j\cos\phi/R^2L)s,$$

$$b_{57} = -(6\sin\phi/RL^3)(L-s)s + (j^2/R^2L^3)(3L-2s)s^2,$$

$$b_{58} = (\sin\phi/RL^2)(2L-3s)s - (j^2/R^2L^2)(L-s)s^2,$$

$$b_{62} = -(3\cos\phi/4RL)[(\sin\phi/R)(L-s) + 1],$$

$$b_{63} = -(j\sin\phi/R^2L^3)(L-s)^2(L+2s) - (6j/RL^3)(L-s)s,$$

$$b_{64} = -(j\sin\phi/R^2L^2)(L-s)^2 s + (j/RL^2)(L-3s)(L-s),$$

$$b_{66} = (3\cos\phi/4RL)[-(\sin\phi/R)s + 1],$$

$$b_{67} = -(j\sin\phi/R^2L^3)(3L-2s)s^2 + (6j/RL^3)(L-s)s,$$

$$b_{68} = (j\sin\phi/R^2L^2)(L-s)s^2 - (j/RL^2)(2L-3s)s.$$